Species richness in North Atlantic fish: Process concealed by pattern

Gislason, Henrik; Collie, Jeremy; MacKenzie, Brian R.; Nielsen, Anders; de Fatima Borges, Maria ; Bottari, Teresa; Chaves, Corina; Dolgov, Andrey V.; Dulcic, Jakov; Duplisea, Daniel; Fock, Heino O.; Gascuel, Didier; de Sola, Luis Gil; Hiddink, Jan Geert; ter Hofstede, Remment; Isajlovic, Igor; Pall Jonasson, Jonas; Jorgensen, Ole; Kristinsson, Kristjan; Marteinsdottir, Gudrun; Masski, Hicham; Matić-Skoko, Sanja; Payne, Mark R.; Peharda, Melita; Reinert, Jakup; Sólmundsson, Jon; Silva, Cristina; Stefansdottir, Lilja; Velasco, Francisco; Vrgoc, Nedo

Global Ecology and Biogeography

DOI:
10.1111/geb.13068

Published: 01/05/2020

Peer reviewed version

Title

The explanatory power of metabolic, neutral and descriptive models of fish species richness in the northern Atlantic

Running Title

Fish species richness

Abstract

Aim Previous analyses of marine fish species richness based on presence-absence data have shown changes with latitude and average species size, but little is known about the underlying processes. To elucidate these processes we use metabolic, neutral and descriptive statistical models to analyse how richness responds to maximum species length, fish abundance, temperature, primary production, depth, latitude, and longitude, while accounting for differences in species catchability, sampling effort and mesh size.

Data Results from 53,382 bottom trawl hauls representing 50 fish assemblages.

Location The northern Atlantic from Nova Scotia to Guinea.

Time period 1977-2013

Methods A descriptive Generalised Additive Model was used to identify functional relationships between species richness and potential drivers, after which non-linear estimation techniques were used to parameterise 1) a 'best' fitting model of species richness built on the functional relationships,

2) an environmental model based on latitude, longitude and depth, and mechanistic models based on 3) metabolic and 4) neutral theory.

Results In the 'best' model the number of species observed is a lognormal function of maximum species length. It increases significantly with temperature, primary production, sampling effort and abundance, and declines with depth and, for small species, with the mesh size in the trawl. The 'best' model explains close to 90% of the deviance and the neutral, metabolic, and environmental models 89%. In all four models, maximum species length and either temperature or latitude account for more than half of the deviance explained.

Main conclusion The two mechanistic models explain the patterns in demersal fish species richness in the northern Atlantic almost equally well. A better understanding of the underlying drivers is likely to require development of dynamic mechanistic models of richness and size evolution, fit not only to extant distributions, but also to historical environmental conditions and to past speciation and extinction rates.

Introduction

Although much has been learned about the richness and distribution of marine species, a mechanistic understanding of the processes responsible for generating and maintaining species richness over evolutionary timescales remains elusive. There is no generally accepted theory to explain the spatial distribution of marine species richness and no general understanding of why some species are more abundant than others (Fine, 2015). This lack of understanding is somewhat surprising. Strong latitudinal gradients in species richness are observed at global and regional scales and these often correlate significantly with environmental variables and life-history traits. Hillebrand (2004) conducted a meta-analysis of gradients in marine biodiversity and found significant relationships between marine species richness, latitude, and species size, while Tittensor et al. (2010) found water temperature to be the main environmental predictor of species richness across a number of marine taxonomic groups. Why latitude, temperature and species size are important is unclear, but size and maximum body size influence the trophic position, mortality, growth and reproduction of many marine species (Andersen et al., 2016), temperature affects their metabolism and food uptake (Gillooly, Brown, West, Savage & Charnov, 2001), and latitude determines the amplitude of the seasonal changes in solar energy input affecting primary production, average temperature and annual temperature range (Cullen, Franks, Karl & Longhurst, 2002).

Bony fish and elasmobranchs are among the best taxonomically resolved groups of marine animals and are therefore well suited for studies of marine species richness. Estimates suggest that on a

55 global scale around 79% of the species have now been described (Mora, Tittensor & Myers, 2008) and
56 very few species have been declared extinct due to human activities (Davies & Baum, 2012). However,
57 most inventories of fish species richness are based on single recordings of individuals with little
58 consideration of differences in individual density and sampling effort. Including density and sampling
59 effort is important for at least two reasons. The number of species recorded is known to depend
60 statistically on the number of individuals and number of samples examined (Gotelli & Colwell, 2001),
61 and high-density areas may have higher species richness because they harbor more individuals able to
62 maintain a higher number of viable populations (Brown, 2014). Based on species inventories,
63 MacPherson & Duarte (1994) found fish species richness and average maximum fish species size to
64 increase with depth and decline with latitude in the northern Atlantic and Fisher, Franks & Leggett
65 (2010) found the geometric mean fish species size to co-vary with species richness. While Blowes,
66 Belmaker & Chase (2017) found the latitudinal change in reef fish richness to scale with abundance,
67 no one has so far analysed how species richness of marine fish found on soft or sandy bottoms is
68 related to density or abundance on a basin-wide scale.
69
70 To understand how fish species richness in different fish communities is related to density or
71 abundance, species length, and environmental conditions, we analyse an extensive dataset,
72 generated by collating results from 31 standardised bottom trawl surveys from the continental
73 shelves of the northern Atlantic and adjacent areas (Figure 1). Our analysis is based on 123 million
74 individual demersal or benthopelagic fish caught in 53 thousand hauls taken within a total survey area
75 of 3.1 million km^2. Bottom trawl surveys are often stratified to account for spatial or depth related

differences in fish assemblage composition and density. We retain the stratification used in the surveys, correct for differences in catchability, and further stratify species into log maximum species length intervals. Using a Generalised Additive Model (GAM) to identify significant variables and relationships we construct a 'best' descriptive model of the number of species caught per log maximum species length interval and survey stratum by transforming the significant relationships identified by the GAM into functional relationships. We also fit an environmental model to the data in which latitude, longitude, depth, total catch and mesh-size are used as independent variables without invoking any biological hypotheses. Using the two descriptive models as reference points we investigate how well mechanistic equilibrium models of species richness based on metabolic (Allen, Brown & Gillooly, 2002; Allen & Gillooly, 2007) and neutral theory (Hubbell, 2001) fit the survey data. Both theories explain the present difference in species richness among fish communities from individual density or abundance, and from fundamental evolutionary processes such as speciation, dispersal and extinction. Recently, they have been combined and used to simulate the latitudinal gradient in species richness in the ocean (Tittensor & Worm, 2016; Worm & Tittensor, 2018).

In brief, the basic assumption of metabolic theory is that temperature enhances species richness by increasing mutation rates and reducing generation times, while extinction rates are inversely related to the average density per species. In contrast to metabolic theory, neutral theory includes a spatial component and assumes that richness is determined by local abundance and random extinctions among functionally equivalent species counterbalanced by immigration from a surrounding meta-community where speciation takes place. Functionally equivalent species are defined as species that

share the same probabilities of death and reproduction (see Appendix S0 in Supporting Information for further information on the two models). Because natural mortality and reproductive output depend on body size in fish, we follow Reuman, Gislason, Barnes, Mélin & Jennings (2014) and assume that functional equivalence, primarily applies for species of similar maximum length. We therefore treat each maximum species length group separately. Comparing the results from the neutral and metabolic models with the two descriptive models, our aim is to elucidate the mechanisms behind the richness differences we observe across fish communities in the northern Atlantic.

Methods

Survey data

Average catch in number of individuals per species and haul was provided from 31 scientific bottom trawl surveys. The time period from which data was obtained from each survey was selected to provide temporal overlap between the surveys and as long a time period from each survey as feasible to minimise the influence of random fluctuations in recruitment and population abundance. Surveys with less than eight years of data were hence excluded. Although the earliest trawl hauls were taken in 1977 and the most recent in 2013, the period from 2001 to 2006 was covered by all surveys. Slightly more than half of the surveys took place in the period from October to March, a third in the period from April to September, and the remaining surveys included hauls obtained throughout the year (See Appendix S1 Table S1.1 in Supporting Information). Different bottom trawls were used in

the surveys. Cod-end mesh sizes ranged from 13 to 40 mm, horizontal trawl openings (wing spread) from 13 to 28 m, vertical openings from 1.9 to 7 m, and towing speeds from 3 to 4.5 knots. Many of the surveys used a stratified random sampling design to account for spatial and depth related differences in species composition. We retained the major strata used in the surveys providing us with richness and density data from 50 different strata. The average depth in these strata ranged from 28 to 950 m.

Environmental data

Sea surface temperature, average temperature in the upper 200 m of the water column, and near bottom temperatures (Kelvin) were obtained from the World Ocean Atlas 2013 (Locarnini et al., 2013) based on decadal average temperature at 0.25° resolution covering the period 1955-2012 for annual, boreal summer (Jul-Sep) and boreal winter (Jan-Mar). Bottom temperatures were defined as the temperature in the layer closest to the bottom. Spatial averages were calculated for each survey stratum, and the seasonal amplitude calculated as the difference between summer and winter values. Estimates of depth integrated pelagic net primary production (npp, $gCm^{-2}y^{-1}$) based on the satellite-derived Vertically Generalised Production Model (VGPM) (Behrenfeld & Falkowski, 1977) were downloaded from www.science.oregonstate.edu/ocean.productivity at 1/12 degree monthly resolution for the period 2002-2012, from which estimates of mean annual npp were derived for each survey area. Latitude and longitude were calculated as the average of the minimum and maximum coordinates of each survey. Average depth was calculated as the midpoint of the depth range of each stratum (see Appendix S1 Table S1.1).

Fish species data

Among the fish taxa recorded some individuals had not been identified to species. If possible, we allocated these individuals to species, assuming that their relative species composition would be identical to that of the individuals identified within the same survey stratum, and family or genus. Where no species from the family or genus had been identified in a stratum, the family or genus name was retained. Information about the maximum length of each species was downloaded from FishBase (Froese & Pauly, 2016) and used to bin the observations into 11 log maximum length intervals of equal width (from now on denoted log maximum length groups). In 1% of the species records no maximum species length was available. These records were excluded from further calculations.

To estimate absolute fish density and abundance in a given stratum or area we first calculated swept area density for each species. This was done by dividing the average number of individuals caught per haul by the average area swept per haul, estimated by multiplying the wing spread of the trawl by the average distance covered per haul. Swept area abundance was calculated by multiplying swept area density by the size of the survey area. Swept area density and abundance can be converted to absolute density and abundance if catchability is known. Catchability, the fraction of the population in the path of the trawl that is retained and caught by the gear, can be estimated by dividing the swept area estimate of abundance by the absolute abundance provided by a stock assessment. Catchability is likely to differ between areas and species and depends on a number of factors including the

properties of the trawl and species-dependent traits such as the size, behavior and distribution of the individuals (Arreguín-Sánchez, 1996; Walker, Maxwell, Le Quesne & Jennings, 2017). To account for differences in horizontal and vertical distribution we sorted the species into: 1) species whose main distribution is outside the main depth range of the surveys (species mainly occurring in the infra-littoral zone and bathy-demersal or bathy-pelagic species found mainly at more than 200 m of depth), and species whose main distribution is inside the main depth range of the surveys, but either 2) mostly occur on either untrawlable grounds (species that are mainly found associated with reefs or in rocky areas), 3) are likely to have a low catchability (species that bury in the sediment, and pelagic species), or 4) are likely to be regularly retained by the survey gear when available (species resting on the seabed, species found close to but not on the seabed, and midwater species with some bottom contact).

We were able to identify 56 cases where catchability could be derived for the species, time period, and area covered by the survey data (see Appendix S2 and Table S2.1 in the Supporting Information). No catchability estimates could be derived for bathy-pelagic and bathy-demersal stocks, and few estimates could be obtained for infra-littoral species, for species mainly found associated with reefs or in rocky areas, and for burying and pelagic species; species that are likely to be under-sampled by the trawl surveys. The average catchability of these species was only 0.05, while the average catchabilities of the species in group four were 0.34, 1.04 and 0.52 for species that were resting on the seabed, found close to the seabed, or found in midwater, respectively. Note that for some of the species found close to the seabed the estimated catchability exceeded 1.0, probably due to their

response to the herding effect of the bridles, sweeps and doors of the trawl. Due to the few and low catchability estimates available for groups two and three, we decided to use only species from group four in our analysis. To extrapolate the 41 catchability estimates available for the 412 species in this group we fitted a log-linear mixed model to the estimates, using the vertical position of the species (resting on seabed, found close to but above the seabed, or midwater with some bottom contact) as a fixed variable and species identity and survey area as random factors. Drawing samples at random from the resulting stochastic model we generated 1000 estimates of catchability for each combination of species and survey stratum (see Appendix S2). The catchabilities were used to calculate average absolute density and abundance in each survey stratum for each of the species found in the surveys. Average absolute density and abundance were finally cumulated across species within each log maximum length group and survey stratum and used as input to the models.

To confirm that the richness of the species in group four had been reasonably well sampled by the surveys we furthermore used the vegan package (Oksanen et al., 2019) to estimate the number of unobserved species in each survey stratum and found that on average a minimum of 7-8% of the species in a particular stratum may not have been recorded. However, considering all of the species found across the surveys few species appear to have been missed (see Appendix S3, Table S3.1 in Supporting Information).

Selection of independent variables

The number of species recorded in a survey stratum is likely to provide a biased estimate of species richness because it depends on the number of individuals caught and identified (the species accumulation curve); the total area swept by the trawl (a measure of sampling effort); the size of the survey stratum (because large strata may contain a larger diversity of environmental conditions and habitats than small); and the mesh-size of the trawl (influencing the proportion of small individuals and species in the catch). To account for the bias we included all four variables in the GAM model. We used the total area swept in each survey stratum rather than the total number of hauls to represent sampling effort because the average duration of the trawl hauls ranged from 15 minutes to one hour across surveys.

According to the metabolic and neutral models, richness should depend on temperature, species size, and either density or absolute abundance. Temperature may influence richness by affecting fish metabolism, generation time and mutation rate, but vary seasonally depending on latitude and longitude and with depth. Identifying the biologically relevant ambient temperature for a fish species is therefore difficult. Average sea surface temperature may be relevant for the pelagic eggs and larvae, average bottom temperature describes the average ambient temperature encountered by the juveniles and adults at the depth where they are caught by the survey trawls, and average temperature in the upper 200 m of the water column may represent the average temperature encountered during the entire life cycle. We furthermore found more than a third of pairwise comparisons of the potential independent variables to be significantly correlated (See Appendix S1 Figure S1.2). Sea surface temperature, bottom temperature and water column temperatures were

highly significantly correlated with each other and with both latitude and longitude, while the seasonal temperature range in the upper 200 m of the water column was significantly correlated to the seasonal temperature ranges near the bottom and at the surface. Net primary production decreased with latitude and increased with temperature, with both correlations highly significant. The vertical opening of the gear was highly significantly correlated to both latitude and to all three temperatures, but not to longitude, reflecting that surveys in high latitudes generally use larger trawls with larger vertical openings than surveys in low latitudes. Total area swept and total stratum area were also highly significantly positively correlated, reflecting that more hauls typically had been taken in large survey strata than in small. Finally, both catch in numbers, average abundance and total swept area were significantly correlated.

Identifying functional relationships

To find the 'best' descriptive model we used a Generalised Additive Model (GAM; Wood, 2006) to identify the functional form and error structure of the relationship between the number of species caught per log maximum length group and the independent variables using the R-package mgcv ver. 1.8.22. In the GAM the log of the expected mean number of species caught, $\mu_{i,j}$, in survey stratum i, maximum length group j, was described using:

$$\log(\mu_{i,j}) = \alpha + s_1(temp\_range_i) + s_2(temp_i) + s_3(abundance_{i,j}) + s_4(depth_i) + s_5(npp_i) + s_6(asurv_i) + s_7(lml_j) + s_8(catch_{i,j}) + s_9(aswept_i) + s_{10}(vertop_i) + s_{11,j}(mesh_i)$$

where α is a proportionality constant; suffix i and j signify survey stratum and maximum length group, respectively, $temp\_range_i$ is the intra-annual temperature range in the stratum (Kelvin); $temp_i$ is temperature (Kelvin); $abundance_{i,j}$ is the average absolute abundance of fish of maximum length j in stratum i ; $depth_i$ is depth (m); npp_i is annual net primary production (gC m^{-2} y^{-1}); $asurv_i$ is the total stratum area (km^2); lml_j is midpoint of log maximum length group (cm); $catch_{i,j}$ is the total number of fish caught in stratum i, maximum length group j over the time period of the survey; $aswept_i$ is area swept by the survey trawl (km^2); $mesh_i$ is mesh-size (mm); and $vertop_i$ is the vertical opening of the trawl (m). The $s_1, \ldots, s_{10}$ are general spline smoothers, while $s_{11,j}$ denotes that for each log maximum length group, j, a separate spline smoother was applied to describe the effect of mesh-size on the number of species caught. The $temp_i$ and $temp\_range_i$ variables were either sea surface, average upper 200 m water column or bottom temperature or were replaced by latitude, lat_i, and longitude, lon_i, when the effect of geographic location was examined, and $abundance_{i,j}$ was changed to $density_{i,j}$ to examine which of the two would provide the best fit.

We used thin plate regression splines with a basis dimension of four as smoothers and a log link. Latitude, longitude, sea surface temperature, bottom temperature, and temperature in the water column were highly significantly correlated, and so were absolute abundance and density. To account for these correlations, we analysed the effect of including these parameters in separate model versions using residual plots and estimates of concurvity (a non-linear analogue of multi-collinearity) to select the best fitting parameter combinations, and AIC-values to identify the most parsimonious model. Model terms were selected by backwards removal of insignificant variables, after which co-

variates generating an estimated concurvity larger than 0.80 were sequentially removed to reduce variance inflation and avoid bias. Distributions of residuals were visually inspected for normality and plotted against each co-variate to reveal heteroscedasticity. We compared models with Poisson and negative binomial error distributions, and found the two to provide an almost equally good fit to the data based on AIC-values and comparisons of the observed and theoretically expected variance, where the importance of over-dispersion was assessed by dividing the sum of squared residuals by the sample size minus the number of parameters estimated (Hilbe, 2011). For the negative binomial model this produced a variance ratio of 0.94, confirming the appropriateness of a negative binomial assumption.

We simplified the GAM model and further reduced its AIC value by inserting the functional relationships indicated by the significant GAM smoothers (see Figure 3). To model the effect of temperature, we assumed that the relationship between species richness and temperature would follow the Arrhenius equation (Gillooly et al., 2001) and consequently used the inverse of temperature in the model. The functional relationships included logarithmic transformations of several of the other independent variables and the addition of a second-order polynomial to capture the change in log species richness with log maximum length. All log transformations used natural logarithms. Using log transformations meant either that zero observations had to be excluded, or that a small positive number had to be added to avoid having to calculate the log of zero. When zero individuals had been caught in a given stratum and log maximum length group, we therefore used the inverse of the total area swept in the stratum to provide a tentative estimate of its maximum density

in the stratum. As evidenced by the residuals, this introduced a small bias in the fit (see Appendix S4, Figure S4.3). Because the neutral model cannot easily be linearised, we used non-linear techniques to estimate the parameters of the four models presented below. This also allowed us to retain the zeros and removed the source of the bias in the GAM model.

Best descriptive model

The significant independent variables in the linearised GAM model were used to construct a 'best' non-linear descriptive model of the number of species caught. The 'best' non-linear model followed the simplified GAM equation and contained an Arrhenius expression where β_2, the 'activation energy of metabolism' (Gillooly et al., 2001), was divided by average water column temperature (Kelvin) multiplied by Boltzmanns constant, k (8.62×10^{-5} eV K^{-1}). It also contained the catch in numbers, the area swept by the trawl, and a mesh-size/log maximum length interaction, total abundance, depth, annual net primary production, and a quadratic log maximum length term, $\exp\left(lml_j + \beta_7\, lml_j{}^2\right)$, to capture the unimodal relationship between species richness and log maximum length:

$$\mu_{i,j} = \alpha * \exp\left(\frac{-\beta_2}{k * temp_i}\right) * abundance_{i,j}{}^{\beta_3} * depth_i{}^{\beta_4} * npp_i{}^{\beta_5} * \exp\left(lml_j + \beta_7\, lml_j{}^2\right) * catch_{i,j}{}^{\beta_8} * aswept_i{}^{\beta_9} * mesh_i{}^{\beta_{11,j}}$$

where α, the proportionality constant, subsumes the combined effects of the standardisation of the Arrhenius expression to a reference temperature, and other pre-factors related to abundance, depth, net primary production, the maximum length term, catch in numbers, area swept and mesh-size.

306

307 Environmental model

308 The environmental model assumes that the number of species observed in survey stratum, i, log
309 maximum length group, j, can be calculated from species richness, described by a simple function of
310 latitude, longitude, depth and log maximum length, corrected for differences in catch in numbers,
311 area swept and mesh-size:

312

313 $$\mu_{i,j} = \alpha * lat_i^{\beta_0} * lon_i^{\beta_1} * {depth_i}^{\beta_4} * \exp\left(lml_j + \beta_7 {lml_j}^2\right) * {catch_{i,j}}^{\beta_8} * {aswept_i}^{\beta_9} * {mesh_i}^{\beta_{11,j}}$$

314

315 Metabolic model

316 In the Metabolic Theory of Ecology, temperature and body size influence the rate of per capita
317 speciation in the same way as they influence metabolism (Gillooly & Allen, 2007) (see Appendix S0).
318 Combining absolute density with a per capita rate of speciation determined by maximum length and
319 temperature provides the speciation rate. In the equilibrium situation, speciation is counterbalanced
320 by extinction, assumed to decline linearly with the average density per species. We added the effect
321 of differences in number of individuals caught, area swept and trawl mesh-size to the model of Segura
322 et al. (2015) to describe the number of species caught:

323

324 $$\mu_{i,j} = \alpha * \exp\left(\frac{-\beta_2}{k * temp_i}\right) * {density_{i,j}}^{\beta_3} * {ml_j}^{\beta_6} * {catch_{i,j}}^{\beta_8} * {aswept_i}^{\beta_9} * {mesh_i}^{\beta_{11,j}}$$

325

where β_2 is the 'activation energy of metabolism' (Gillooly & Allen, 2007), k is Boltzmann's constant, ml_j is the median maximum length of the species in log maximum length group j, and α, the proportionality constant, accounts for the combined effects of the standardisation of the Arrhenius expression to a reference temperature, as well as other pre-factors related to the density term, and to the maximum length, catch in numbers, area swept and mesh-size terms.

Neutral model

According to the Neutral Theory of Biodiversity and Biogeography, the number of functionally equivalent species in a local community is determined by random extinctions caused by ecological drift, counterbalanced by immigration of species from a larger surrounding meta-community where random speciation takes place (Hubbell, 2001; Rosindell, Hubbell & Etienne, 2011) (see Appendix S0).

Following Reuman et al. (2014), we assume that species of similar log maximum length are functionally equivalent and model each log maximum length group separately, using the approximate formula derived by Etienne & Olff (2004) and Reuman et al. (2014) to describe the relative number of species in each survey stratum and log maximum length group. We also assume that the probability of immigration, λ, is independent of stratum area, but allow it to vary with log maximum length. To account for the effect of differences in the number of individuals examined, effort and sampling gear on the number of species caught, we add number of individuals caught, total area swept and mesh-size terms to the species richness model of Reuman et al. (2014) providing the following equation:

$$\mu_{i,j} \approx J_{M_j} * \left(\frac{\nu_i}{1-\nu_i}\right) * \log\left[1 - \frac{\lambda_j\, log(\lambda_j)}{1-\lambda_j} * \left(\frac{abundance_{i,j}}{J_{M_j} * (\nu_i/(1-\nu_i))}\right)\right] * {catch_{i,j}}^{\beta_8} * {aswept_j}^{\beta_9} * mesh_i^{\beta_{11,j}}$$

Where J_{M_j} is absolute abundance in log maximum length group j in the meta-community, $abundance_{i,j}$ is the absolute abundance of group j in the local community, and ν_i is the per capita speciation rate in area i. Note also that J_{M_j} and ν_i are confounded in the $J_{M_j}(\nu_i/(1-\nu_i))$ term. However, as the speciation rate is likely to be very small, the term can be approximated by the fundamental biodiversity number, $\theta_{i,j} = J_{M_j}\nu_i$ (Rosindell et al., 2011). Because fish evolution is affected by temperature (Wright, Ross, Keeling, McBride & Gillman, 2011), we follow Tittensor & Worm (2016) and make ν_i temperature dependent by adding the Arrhenius equation. Finally, we approximate the change in J_{M_j} with log maximum length by a quadratic term as found in the 'best' descriptive model and thus end up with:

$$J_{M_j}\left(\frac{\nu_{i,j}}{1-\nu_{i,j}}\right) \approx \theta_{i,j} = \alpha * \exp\left(lml_j + \beta_7\, {lml_j}^2\right) * \exp\left(\frac{-\beta_2}{k * temp_i}\right)$$

where α again is an overall proportionality constant. Hence

$$\mu_{i,j} = \theta_{ij} * \log\left[1 - \frac{\lambda_j\, log(\lambda_j)}{1-\lambda_j} * \frac{abundance_{i,j}}{\theta_{ij}}\right] * {catch_{i,j}}^{\beta_8} * {aswept_j}^{\beta_9} * mesh_i^{\beta_{11,j}}$$

where, $j = 1 \ldots 11$, is log maximum length group, i is stratum and $abundance_{i,j}$ is the total number of individuals in stratum i group j estimated by multiplying the size of stratum i with the absolute density of fish in i belonging to log maximum length group j.

Estimating model parameters

We use the non-linear model fitting R-package TMB (Kristensen, Nielsen, Berg, Skaug & Bell, 2015) to estimate the parameters of the four non-linear models. Fitting each model to the number of species observed we removed any insignificant variables, except if they were important for the theoretical underpinning of a model. We visually inspected the Pearson residuals of each model for normality and plotted them against each co-variate to reveal potential heteroscedasticity. To compare the models we calculated AIC-values (Burnham & Anderson, 2002), R^2 from observed and predicted number of species, and proportion of deviance explained. The latter was estimated by fixing the estimated scale parameter, κ, of the negative binomial distribution used in each of the models, comparing the difference in deviance between a saturated model (with one parameter for each of the 550 observations) and the actual model, to the difference in deviance between a saturated model and a model with only one parameter (Cameron & Windmeijer, 1996). To also illustrate how much of the overall deviance each model term explained, we consecutively replaced each of the independent variables by its overall average and calculated the relative increase in the proportion of deviance explained when the actual observations were used instead of the average. Having identified the four most parsimonious models we examined their sensitivity to the uncertainty in the abundance and density data by fitting them to the 1000 separate estimates of density and abundance obtained from

387 the mixed effects catchability model, and calculated the mean and variance of the resulting
388 parameter estimates. We plotted the proportion of the deviance explained by each of the model
389 parameters in the 1000 runs, and used these to illustrate the sensitivity of our results to the
390 uncertainty in the catchability estimates. All analyses were undertaken in R version 3.4.4.
391
392
393 Results
394
395 Observed number of species and density
396 The number of observed species, log average swept area density, and log average absolute density
397 follow almost symmetrical distributions when plotted against log maximum length (Figure 2). As
398 expected, the average number of species observed increases with temperature while log average
399 swept area density and log average absolute density change little except in areas with a mean annual
400 sea temperature below 7.5°C where the densities are significantly lower in the intermediate length
401 range.
402
403 GAM model
404 Fitting the GAM to the survey data reveals a strong and highly significant unimodal effect of log
405 maximum length on log number of species observed, a significant effect of absolute fish abundance,
406 significant non-linear positive effects of average temperature in the upper 200 m of the water column
407 and area swept, and a significant positive linear effect of net primary production. Log number of

species caught declines significantly with depth and, for the smaller length groups, with increasing mesh-size (Figure 3). Stratum area, vertical opening, temperature range and catch in numbers were all insignificant or generated a too high concurvity. The model explains 85% of the deviance, and has a lower AIC than model versions in which abundance is replaced by density and average temperature by either sea surface temperature, bottom temperature, or latitude and longitude. Although there are survey strata that produce significant negative residuals, such as the 50-200m stratum in Guinea which features the lowest number of hauls of all strata, there are no clear patterns in the residuals across survey strata. This suggests that the model provides an equally good description of fish species richness in the Atlantic, Arctic and Mediterranean Seas (Figure 4). Further model diagnostics are shown in Appendix S4, Figures S4.1 and S4.2).

Some of the smooth relationships suggested that the AIC value could be further reduced by using the logarithm or the inverse of the independent variable, and for log maximum length, in particular, that the smoother could be replaced by a second-order term, corresponding to a log-normal like distribution of richness versus maximum length. Replacing the independent variables in the GAM by inverse temperature, log abundance, log depth, net primary production, log area swept, an interaction between mesh-size and log maximum length, and the exponential of a second-order polynomial in log maximum length, reduced the AIC-value from 2090 to 1860 and increased the percentage of deviance explained to 91%.

Non-linear models

We use non-linear estimation techniques to compare the 'best' descriptive model identified by the GAM to the three other models. Fitting the four models to the average absolute densities and abundances we initially used variance ratio tests to determine whether the bias correcting terms ($catch_{i,j}{}^{\beta_8}$, $aswept_j{}^{\beta_9}$ and $mesh_i^{\beta_{11,j}}$) contributed significantly to the fit. We found that $catch_{i,j}{}^{\beta_8}$ did not improve the fit of the 'best' and neutral models significantly, improved the metabolic model marginally, but contributed highly significantly to the fit of the environmental model. The total area swept, $aswept_j{}^{\beta_9}$, contributed significantly to all models, except the environmental, while the term reflecting the interaction between mesh size and maximum length, $mesh_i^{\beta_{11,j}}$, was significant in all four models. In the neutral model the per capita immigration rates, λ_j, were not significantly different from zero; and were therefore replaced by a single overall λ for all log maximum length groups (see Appendix S4 Table S4.1).

Fitting the 'best' model to the average of the absolute abundances explains 90% of the deviance (Table 1). The neutral model provides the second-best fit (ΔAIC=38) followed by the metabolic model (ΔAIC=40) and the environmental model (ΔAIC=46). Note that the difference between the metabolic and neutral models can be explained by the additional parameter included in the former. Many of the parameter estimates are similar across models. The interaction between log maximum length and mesh-size, $\beta_{11,j}$, is thus negative for the smaller species in all models, implying a general decline in the number of small species caught as mesh-size increases. In all models log maximum length and either temperature or latitude account for most of the deviance explained (Figure 5). The parameter estimates of 'best', metabolic and neutral models are robust to the uncertainty in the modelled

450 catchabilities as shown by the limited distribution of deviance around the mean value of the 1000
451 estimates. The standard deviations of the parameter estimates are also small (see Appendix S4 Table
452 S4.1). Additional model diagnostics are presented in the Supplementary Information (Appendix S4
453 Figures S4.4 & S4.5).
454
455
456 Discussion
457
458 Our study reveals strong consistent patterns in the number of demersal and benthopelagic fish
459 species across the northern Atlantic. As in previous investigations, we find body size, depth and either
460 temperature or latitude to be important, but our analysis is the first in which differences in the
461 number of individuals caught, area swept and mesh-size are considered, and where net primary
462 production and absolute fish abundance or density are used as covariates. We find fish species
463 richness to increase with temperature, fish abundance, and net primary production, but to decline
464 with depth and latitude. Adjusting for differences in area swept and mesh-size, the 'best' descriptive
465 model explains 90% of the deviance in the number of species caught by log maximum length,
466 temperature, fish abundance, depth and primary production (Table 1). The neutral model in which
467 inverse temperature, a parabolic relationship with log maximum length, area swept and mesh-size are
468 significant, explains 89% of the deviance, and so does the metabolic model. Our analyses furthermore
469 show that both the neutral and metabolic models provide significantly better fits than the

environmental model in which local richness is described as a function of log maximum length, catch, latitude, longitude and depth.

In all four non-linear models more than half of the deviance is explained by a combination of log maximum length and either temperature or latitude (Figure 5). In the data the distribution of the number of species observed across maximum length groups is approximately lognormal (Figure 2). Similar distributions have been obtained for marine bivalves (Roy, Jablonsky & Martien, 2000), terrestrial snakes (Boback & Guyer, 2003), and insects (Siemann, Tilman & Haarstad, 1996), while more right-skewed distributions have been found for birds and mammals (Purvis, Orme & Dolphin, 2003; Smith & Lyons, 2013). A lognormal distribution also provided a highly significant fit in the best, neutral and environmental models (Table 1). Contrary to this, metabolic theory predicts that species richness should scale with body mass raised to a power of 0.75, hence maximum length to a power of 2.25. This prediction was not confirmed by our analysis where the power was estimated to -1.00 (±0.48 conf. lim.) and thus highly significantly different from the expected.

The average water column temperature from 0-200 m is a better predictor of the observed number of fish species than bottom temperature, surface temperature and latitude. Latitude and average temperature are negatively correlated, but the correlation breaks down at intermediate latitudes, where average temperature generally is higher in the eastern part of the northern Atlantic due to the influence of the Gulf Stream. The increase in the number of fish species caught with temperature seems to be well described by the Arrhenius equation. Metabolic theory emphasizes the role of

491 temperature and body size on mutation rate and generation time, and it is interesting that the
492 Arrhenius constant, β_2, is 0.47 (± 0.06 conf. lim.) and 0.52 eV (±0.06 conf. lim.), respectively, in the
493 metabolic and neutral models. This range is not far from the average activation energy of metabolism
494 of 0.65 eV predicted by metabolic theory (Gillooly & Allen, 2007; Bailly et al., 2014), and close to
495 empirical estimates of the activation energy of fish metabolism. Clarke & Johnston (1999) and Gillooly
496 et al. (2001) both used the Arrhenius equation to describe the relationship between the resting
497 metabolism of fish and temperature, and independently estimated the activation energy as 0.43 eV.
498 Barneche et al. (2014) used a model with a temperature optimum to account for metabolic
499 inactivation at high temperatures and found an activation energy of 0.59 eV. How temperature
500 influences the rates of speciation and extinction is not completely known, and other co-varying
501 factors may be involved (see e.g. Rabosky et al., 2018).
502
503 The 'best' and neutral models contain positive relationships between abundance and the number of
504 species observed. The 'best' model also includes a significant positive relationship with net primary
505 production. Areas of high productivity have been hypothesised to have higher species richness
506 because they harbor more individuals able to maintain a higher number of viable populations (Brown,
507 2014), although a recent review by Storch, Bodhalkvá & Okie (2018) found the empirical evidence in
508 favor of this hypothesis to be mixed. However, in areas where abundance has been significantly
509 reduced by fishing, primary production may better reflect fish abundance and density in the
510 unexploited state and hence be a better predictor of richness. Without primary production included in
511 the model, the three largest positive differences between the observed and predicted number of

512 species were generated by the data from Mauretania, which features the highest primary production,
513 but has been subject to marked overexploitation (Meissa & Gascuel, 2014). Note however, that
514 abundance or density never accounted for more than 10% of the total deviance in the 'best', neutral
515 and metabolic models, explaining the robustness of these models to the uncertainty in the
516 catchabilities (Figure 5).
517
518 Tittensor & Worm (2016) and Worm & Tittensor (2018) used a neutral model to simulate species
519 richness in the ocean and allowed speciation rate and generation time to depend on temperature.
520 Thermal effects on speciation rate generated a stable but weak latitudinal richness gradient in their
521 model, while thermal effects on generation time produced a transient latitudinal richness gradient
522 that eventually disappeared. Combining the effect of an increase in abundance caused by the increase
523 in ocean area towards the equator and a temperature-dependent speciation rate produced the most
524 realistic gradient in richness. Fitting a neutral model to the survey data we found a strong effect of
525 temperature on species richness and a weaker influence of fish abundance. Furthermore, the shelf
526 areas in the eastern Atlantic down to 200 m, the depth range where our fish species have their
527 maximum abundance, increases with latitude from the Equator to the Arctic (Pilson & Seitzinger,
528 1996). A consistent decline in habitat area with latitude is therefore unlikely to explain our results.
529
530 The parameter describing the probability of immigration in the neutral model could not be estimated
531 with sufficient precision. The known functional dependency between per capita immigration
532 probability and the speciation rate in the surrounding meta-community makes it difficult to estimate

both parameters simultaneously (Jabot & Chave, 2011). The immigration probability may depend on temperature and size, as assumed by Reuman et al. (2014), but the evidence for temperature related differences in larval dispersal is lacking (Leis et al., 2013), and when immigration probability was assumed to be size dependent, none of the estimates of λ_j were significant. Additional analysis of species distributions and information on the genetic divergence of subpopulations is necessary to fully understand the relationship. The neutral model has been criticised for predicting unrealistically long species ages for common species and too short species ages for new species with few individuals (Chisholm & O'Dwyer, 2014). Recent work has shown that more realistic species ages are generated when protracted speciation and weak selection caused by small differences in hereditary fitness are incorporated in the model (Rosindell et al., 2015), but no approximate solution for the number of species in each community is yet available for this model.

Despite the large sample sizes and good geographical coverage of the survey data, several problems may be associated with using bottom trawl survey data to study fish species richness and density patterns. The main aim of a scientific bottom trawl survey is often to provide reliable estimates of the relative abundance and year-class strength of commercially important fish species, and less attention may therefore be given to identifying species that are rare or of little or no commercial value. Trawl-survey catches may furthermore provide biased estimates of the actual fish species composition and density due to species and size-specific differences in the probability of the individuals to be retained by the trawl (Arreguín-Sánchez, 1996). Some species and sizes are herded into the path of the trawl by the action of the otter doors and trawl sweeps, others avoid the trawl by escaping under the

554 fishing line or over the headline, others are able to outswim the trawl, and among those entering the
555 trawl the smaller individuals and species may escape through the meshes. Factors that have been
556 reported to influence the catch efficiency of survey trawls include time of day, light intensity,
557 turbidity, current strength and direction, depth, sweep length, net spread and vertical opening, trawl
558 speed, haul duration, and the size and type of the ground gear (Arreguín-Sánchez, 1996; Fraser,
559 Greenstreet & Piet, 2007). Although we corrected our analysis for differences in species catchability,
560 we were unable to fully account for all of the factors that may lead to species and size specific
561 differences in catchability. This was due to the sparsity of spatially and temporally overlapping stock
562 assessments, the absence of individual length measurements for many of the non-commercial
563 species, and our use of average catch rates rather than individual hauls**.** However, as seen in Figure 5,
564 density or abundance only explain less than 10% of the deviance. The sensitivity of our overall
565 conclusions to the uncertainty in the catchabilities is therefore modest, and the parameter estimates
566 and the relative importance of the variables only change little in the different models. Finally, our use
567 of a single estimate of maximum length for each species hides the fact that maximum body length in
568 fish is likely to vary from area to area (Rypel, 2013). However, the maximum length of a species in a
569 given area is difficult to estimate as it depends on local fishing mortality and sampling effort.
570
571 We base our analysis on the number of fish species and individuals observed over a recent period of
572 time in different regions of the northern Atlantic, Arctic and Mediterranean Seas. It is now well
573 documented that changes in fish distributions have occurred over the last decade or two in many
574 regions of the North Atlantic and that these are significantly associated with changes in temperature,

(Perry, Low, Ellis & Reynolds, 2005; Hiddink & Ter Hofstede, 2008; Batt, Morley, Selden, Tingley & Pinsky, 2017). We have fitted our models to data from a period when temperatures have been increasing, but where regulatory processes generally seem to maintain existing patterns in species richness (Gotelli et al., 2017). Future analyses should investigate whether these patterns will persist over longer time periods and how our model parameters will be modified by temperature change, for example by conducting the analyses on different time periods characterised by different mean temperatures. Such analyses could provide insight into the relative importance of temperature having a direct effect on metabolic processes vs. its effects on other ecosystem features that affect species richness. For example, Marbá, Jordà, Augustí, Girard & Duarte (2015) showed that the activation energy for many biological responses in the Mediterranean Sea is far higher than the reported activation energy for metabolism, suggesting that temperature increases are having additional ecosystem effects on biotic responses beyond their effect on metabolic processes and speciation rates. The effects of global warming on fish communities have been predicted from stacked species distribution models (SSDMs; e.g. Jones & Cheung, 2015), but these models have so far largely ignored the regularity in the distribution of fish species richness and abundance with log maximum length. This regularity accounts for a third or more of the deviance explained by our models (Figure 5) and may thus be used to improve the predictive capability of the SSDMs significantly. But while the right-hand side of the richness versus log maximum length distribution, consisting of species with a maximum length larger than app. 50 cm, has been explained by size spectrum theory (Reuman et al., 2014), little is known about the processes shaping the left-hand side.

596 Numerous hypotheses have been put forward to explain the latitudinal pattern in species richness
597 (Brown, 2014; Fine, 2015). Finding log maximum length, temperature, absolute fish abundance, depth
598 and net primary production to explain 90% of the deviance in the distribution of demersal fish species
599 richness across the northern Atlantic, and both neutral and metabolic equilibrium models to explain
600 close to 89%, conveys an important message. When 89% of the deviance in the extant species
601 richness can be explained by two competing mechanistic hypotheses, and by a model based on
602 latitude, longitude and depth, and when many of the independent variables are significantly
603 correlated, it seems relevant to question how much more the present patterns in species richness and
604 abundance can tell us about the underlying environmental, ecological and evolutionary processes
605 (Gotelli et al., 2009). We probably need dynamic mechanistic models with more realistic descriptions
606 of speciation, dispersal and extinction plus additional data to reveal how past changes in
607 environmental (e.g. temperature, currents, ice cover, shelf area) and biotic (e.g. primary production)
608 variables may have contributed to shaping the present distribution of species richness and the strong
609 lognormal relationship between richness and maximum length (Fine, 2015; Descombes et al., 2018).
610 Such data should include information from paleo-geographical and climatological reconstructions of
611 past environmental conditions as well as information about body size evolution, diversification rates
612 and species lifetimes from molecular phylogenetics and the fossil record (Romano et al., 2016; Alfaro
613 et al., 2018). In addition to providing a baseline from which we can evaluate future change, our data
614 and results point to new possibilities for understanding demersal fish species biogeography in the
615 northern Atlantic.
616

617

618 References

619 Alfaro, M.E., Faircloth, B.C., Harrington, R.C., Sorenson, L., Friedman, M., Thacker, … Near, T.J., 2018.
620 Explosive diversification of marine fishes at the Cretaceous-Palaeogene boundary. *Nature*
621 *Ecology and Evolution*, 2, 688-696.

622 Allen, A.P., Brown, J.H. & Gillooly, J.F., 2002. Global biodiversity, biochemical kinetics, and the
623 energetic-equivalence rule. *Science*, 297, 1545-1548.

624 Allen, A.P., & Gillooly, J.F., 2007. The mechanistic basis of the metabolic theory of ecology. *Oikos,*
625 116, 1073-1077.

626 Andersen, K.H., Berge, T., Gonçalves, R.J., Hartvig, M., Heuschele, J., Hylander, S., ... Olsson, K., 2016.
627 Characteristic sizes of life in the oceans, from bacteria to whales. *Annual Review of Marine*
628 *Science*, 8, 217-241.

629 Arreguín-Sánchez, F., 1996. Catchability: a key parameter for fish stock assessment. *Reviews in Fish*
630 *Biology and Fisheries*, 6, 221-242.

631 Bailly, D., Cassemiro, F.A., Agostinho, C.S., Marques, E.E. & Agostinho, A.A., 2014. The metabolic
632 theory of ecology convincingly explains the latitudinal diversity gradient of Neotropical
633 freshwater fish. *Ecology*, 95, 553-562.

634 Barneche, D.R, Kulbicki, M., Floeter, S.R., Friedlander, A.M., Maina, J., & Allen, A.P., 2014. Scaling
635 metabolism from individuals to reef-fish communities at broad spatial scales. *Ecology Letters*,
636 17, 1067-1076.

637 Batt, R.D., Morley, J.W., Selden, R.L., Tingley, M.W. & Pinsky, M.L., 2017. Gradual changes in range
638 size accompany long-term trends in species richness. *Ecology Letters*, 20, pp.1148-1157.

639 Behrenfeld, M.J. & Falkowski, P.G., 1977. Photosynthetic rates derived from satellite-based
640 chlorophyll concentration. *Limnology and Oceanography*, 42, 1-20.
641 Blowes, S. A., Belmaker, J. & Chase, J. M., 2017. Global reef fish richness gradients emerge from
642 divergent and scale-dependent component changes. *Proceedings of the Royal Society B:*
643 *Biological Sciences*, 284, 20170947.
644 Boback, S.M., & Guyer, C., 2003. Empirical evidence for an optimal body size in snakes. *Evolution*,
645 57, 345-351.
646 Brown, J. H., 2014. Why are there so many species in the tropics? *Journal of Biogeography*, 41, 8-22.
647 Burnham, K.P., & Anderson, D. R., 2002. *Model selection and multimodel inference: a practical*
648 *information theoretic approach*. 2nd ed. Springer, New York, 488pp.
649 Cameron, A.C. & Windmeijer, F.A., 1996. R-squared measures for count data regression models with
650 applications to health-care utilization. *Journal of Business and Economic Statistics*, 14, 209-220.
651 Chisholm, R.A. & O'Dwyer, J.P., 2014. Species ages in neutral biodiversity models. *Theoretical*
652 *Population Biology*, 93, 85-94.
653 Clarke, A., & Johnston, N.M., 1999. Scaling of metabolic rate with body mass and temperature in
654 teleost fish. *Journal of Animal Ecology*, 68, 893-905.
655 Cullen, J. J., Franks, P. J., Karl, D. M., & Longhurst, A., 2002. Physical influences on marine ecosystem
656 dynamics. In Robinson A.R., McCarthy, J.J. & Rothschild, B.J. (eds.). *The Sea*, 12, 297-336.
657 Davies, T.D. & Baum, J.K., 2012. Extinction risk and overfishing: reconciling conservation and
658 fisheries perspectives on the status of marine fishes. *Scientific reports*, 2, p.561.

Descombes, P., Gaboriau, T., Albouy, C., Heine, C., Leprieur, F., & Pellissier, L., 2018. Linking species diversification to palaeo-environmental changes: A process-based modelling approach. *Global Ecology and Biogeography*, 27, 233-244.

Etienne, R.S., & Olff, H., 2004. How dispersal limitation shapes species body size distributions in local communities. *The American Naturalist,* 163, 69-83.

Fine, P.V., 2015. Ecological and evolutionary drivers of geographic variation in species diversity. *Annual Review of Ecology, Evolution, and Systematics*, 46, 369-392.

Fisher, J.A., Frank, K.T., & Leggett, W.C., 2010. Global variation in marine fish body size and its role in biodiversity–ecosystem functioning. *Marine Ecology Progress Series*, 405, 1-13.

Fraser, H.M., Greenstreet, S.P. and Piet, G.J., 2007. Taking account of catchability in groundfish survey trawls: implications for estimating demersal fish biomass. *ICES Journal of Marine Science*, 64, 1800-1819.

Froese, R., & Pauly, D., (eds.), 2016. FishBase. World Wide Web electronic publication. www.fishbase.org, version (01/2016).

Gillooly, J.F., Brown, J.H., West, G.B., Savage, V.M., & Charnov, E.L., 2001. Effects of size and temperature on metabolic rate. *Science*, 293, 2248-2251.

Gillooly, J.F., & Allen, A.P., 2007. Linking global patterns in biodiversity to evolutionary dynamics using metabolic theory. *Ecology*, 88, 1890-1894.

Gotelli, N.J., Anderson, M.J., Arita, H.T., Chao, A., Colwell, R.K., Connolly, S.R., … Willig, M.R., 2009. Patterns and causes of species richness: a general simulation model for macroecology. *Ecology Letters,* 12, 873-886.

680 Gotelli, N. J., & Colwell, R. K., 2001. Quantifying biodiversity: procedures and pitfalls in the
681 measurement and comparison of species richness. *Ecology Letters*, 4, 379-391.
682 Gotelli, N.J., Shimadzu, H., Dornelas, M., McGill, B., Moyes, F., & Magurran, A.E., 2017. Community-
683 level regulation of temporal trends in biodiversity. *Science advances*, 3, p.e1700315.
684 Hiddink, J.G., & Ter Hofstede, R., 2008. Climate induced increase in species richness of marine fishes.
685 *Global Change Biology*, 13, 453-460.
686 Hilbe, J.M., 2011. *Negative Binomial Regression*. 2nd ed. Cambridge University Press, 553pp.
687 Hillebrand, H., 2004. Strength, slope and variability of marine latitudinal gradients. *Marine Ecology*
688 *Progress Series*, 273, 251-267.
689 Hubbell, S.P., 2001. *The unified neutral theory of biodiversity and biogeography.* Monographs in
690 Population Biology, Vol. 32. Princeton University Press. 375pp.
691 Jabot, F., & Chave, J., 2011. Analyzing tropical forest tree species abundance distributions using a
692 non-neutral model and through approximate Bayesian inference. *The American Naturalist*, 178,
693 E37-E47.
694 Jones, M.C., & Cheung, W.W.L., 2015. Multi-model ensemble projections of climate change effects
695 on global marine biodiversity, *ICES Journal of Marine Science*, 72,741–752.
696 Kristensen, K., Nielsen, A., Berg, C.W., Skaug, H., & Bell, B., 2015. TMB: automatic differentiation and
697 Laplace approximation. *arXiv preprint arXiv:1509.00660*.
698 Leis, J.M., Caselle, J.E., Bradbury, I.R., Kristiansen, T., Llopiz, J.K., Miller, M.J., ... Swearer, S.E., 2013.
699 Does fish larval dispersal differ between high and low latitudes? *Proceedings of the Royal*
700 *Society of London B: Biological Sciences*, 280, p.20130327.

Locarnini, R. A., Mishonov, A. V., Antonov, J. I., Boyer, T. P., Garcia, H. E., Baranova, … Seidov, D., 2013. World Ocean Atlas 2013, Volume 1: Temperature. S. Levitus, Ed., A. Mishonov Technical Ed.; NOAA Atlas NESDIS 73, 40pp.

Macpherson, E., & Duarte, C. M., 1994. Patterns in species richness, size, and latitudinal range of East Atlantic fishes. *Ecography*, 17, 242-248.

Marbà, N., Jordà, G., Agustí, S., Girard, C., & Duarte, C.M., 2015. Footprints of climate change on Mediterranean Sea biota. *Frontiers in Marine Science*, 2:56 doi: 10.3389/fmars.2015.00056.

Meissa, B., & Gascuel, D., 2014. Overfishing of marine resources: some lessons from the assessment of demersal stocks off Mauritania. *ICES Journal of Marine Science*, 72, 414-427.

Mora, C., Tittensor, D.P., & Myers, R.A., 2008. The completeness of taxonomic inventories for describing the global diversity and distribution of marine fishes. *Proceedings of the Royal Society of London B: Biological Sciences*, 275, 149-155.

Oksanen, J., Blanchet, F.G., Friendly, M., Kindt, R., Legendre, P., ... Wagner, H., 2019. Vegan: Community Ecology Package. R package version 2.2-1.

Perry, A.L., Low, P.J., Ellis, J.R., & Reynolds, J.D., 2005. Climate change and distribution shifts in marine fishes. *Science*, 308, 1912–1915.

Pilson, M.E., & Seitzinger, S.P., 1996. Areas of shallow water in the North Atlantic. Biogeochemistry, 35, 227-233.

Purvis, A., Orme, C.D.L., & Dolphin, K., 2003. *Why are Most Species Small-Bodied?* Macroecology: Concepts and Consequences, pp.155–173. Oxford University Press, Oxford.

721 Rabosky, D.L., Chang, J., Title, P.O., Cowman, P.F., Sallan, L., Friedman, … Alfaro, M.E., 2018. An
722 inverse latitudinal gradient in speciation rate for marine fishes. *Nature*, 55, 392–395
723 Reuman, D.C., Gislason, H., Barnes, C., Mélin, F., & Jennings, S., 2014. The marine diversity
724 spectrum. *Journal of Animal Ecology*, 83, 963-979.
725 Romano, C., Koot, M.B., Kogan, I., Brayard, A., Minikh, A.V., Brinkmann, W., … Kriwet, J., 2016.
726 Permian–Triassic Osteichthyes (bony fishes): diversity dynamics and body size evolution.
727 *Biological Reviews*, 91, 106-147.
728 Rosindell, J., Harmon, L.J., & Etienne, R.S., 2015. Unifying ecology and macroevolution with
729 individual-based theory. *Ecology Letters*, 18, 472-482.
730 Rosindell, J., Hubbell, S.P., & Etienne, R.S., 2011. The unified neutral theory of biodiversity and
731 biogeography at age ten. *Trends in Ecology and Evolution*, 26, 340-348.
732 Roy, K., Jablonski,D., & Martien, K.K., 2000. Invariant size-frequency distributions along a latitudinal
733 gradient in marine bivalves. *Proc. Nat. Acad. Sci.*, 97, 13150–13155.
734 Rypel, A.L., 2013. The cold-water connection: Bergmann's rule in North American freshwater fishes.
735 *The American Naturalist*, 183, 147-156.
736 Segura, A.M., Calliari, D., Kruk, C., Fort, H., Izaguirre, I., Saad, J.F., & Arim, M., 2015. Metabolic
737 dependence of phytoplankton species richness. *Global Ecology and Biogeography*, 24, 472-482.
738 Siemann, E., Tilman, D., & Haarstad, J., 1996. Insect species diversity, abundance and body size
739 relationships. *Nature*, 380, 704-706.
740 Smith, F.A., & Lyons S.K., 2013. *Animal Body Size: Linking Pattern and Process across Space, Time,*
741 *and Taxonomic Group*. University of Chicago Press. 272pp.

742 Storch, D., Bodhalkvá, E., & Okie, J., 2018. The more-individuals hypothesis revisited: the role of
743 community abundance in species richness regulation and the productivity-diversity
744 relationship. *Ecology Letters*, 21, 920-937.
745 Tittensor, D.P., Mora, C., Jetz, W., Lotze, H. K., Ricard, D., Berghe, E. V., & Worm, B., 2010. Global
746 patterns and predictors of marine biodiversity across taxa. *Nature*, 466, 1098-1101.
747 Tittensor, D.P. & Worm, B., 2016. A neutral-metabolic theory of latitudinal biodiversity. *Global*
748 *Ecology and Biogeography*, 25, 630-641.
749 Walker, N. D., Maxwell, D. L., Le Quesne, W. J., & Jennings, S., 2017. Estimating efficiency of survey
750 and commercial trawl gears from comparisons of catch-ratios. *ICES Journal of Marine Science*,
751 74, 1448-1457.
752 Wood, S.N., 2006. *Generalized additive models: an introduction with R*. Boca Raton, Florida:
753 Chapman and Hall/CRC. 391pp.
754 Worm, B., & Tittensor, D.P., 2018. *A Theory of Global Biodiversity*. Monographs in Population
755 Biology 60. Princeton University Press, 214 pp.
756 Wright, S.D., Ross, H.A., Keeling, D.J., McBride, P., & Gillman, L.N., 2011. Thermal energy and the
757 rate of genetic evolution in marine fishes. *Evolutionary Ecology*, 25, 525-530.
758
759
760
761
762

Data accessibility

The data and R-code that support the findings of this study and were used to produce the figures and tables are deposited on GitHub (https://github.com) in the repository 'DTUAqua/biodiversity'.

768 Table 1. Parameter estimates from TMB-model fits using average absolute density and abundance.
769 Standard error in parentheses and significance levels indicated by stars (***=<0.001, **=< 0.01, *=<
770 0.05) (one-sided t-test, n=550). NS= Non Significant term retained in the model fit. NSR= Non
771 Significant term removed from the model.

Parameter		Best descriptive model	Neutral	Metabolic	Environmental
Constant	$(log\alpha)$	16.90 (1.63)***	22.95 (1.35)***	24.89 (1.65)***	3.093 (0.687)***
Latitude	(β_0)				-0.518 (0.055)***
Longitude	(β_1)				0.426 (0.073)***
Temperature	(β_2)	0.322 (0.035)***	0.521 (0.029)***	0.466 (0.029)***	
Abundance	(β_3)	0.034 (0.009)***			
Density	(β_3)			0.056 (0.011)***	
Depth	(β_4)	-0.115 (0.029)***			-0.167 (0.034)***
Net prim. prod.	(β_5)	0.217 (0.045)***			
Max. length	(β_6)			-1.000 (0.246)***	
Log. max. length^2	(β_7)	-0.131 (0.028)***	-0.131 (0.031)***		-0.235 (0.029)***
Immigration	(λ)		NS		
Catch	(β_8)	NSR	NSR	NSR	0.067 (0.010)***
Area swept	(β_9)	0.079 (0.023)***	0.129 (0.022)***	0.176 (0.022)***	NSR
Mesh:mlgr$_{1.5}$	$(\beta_{11,1})$	-1.537 (0.181)***	-1.351 (0.184)***	-1.675 (0.242)***	-1.070 (0.187)***
Mesh:mlgr$_{2.0}$	$(\beta_{11,2})$	-1.378 (0.162)***	-1.205 (0.164)***	-1.421 (0.202)***	-1.021 (0.168)***
Mesh:mlgr$_{2.5}$	$(\beta_{11,3})$	-0.977 (0.120)***	-0.875 (0.124)***	-0.972 (0.143)***	-0.755 (0.125)***
Mesh:mlgr$_{3.0}$	$(\beta_{11,4})$	-0.598 (0.099)***	-0.509 (0.103)***	-0.552 (0.108)***	-0.458 (0.103)***
Mesh:mlgr$_{3.5}$	$(\beta_{11,5})$	-0.401 (0.078)***	-0.335 (0.081)***	-0.347 (0.082)***	-0.340 (0.082)***
Mesh:mlgr$_{4.0}$	$(\beta_{11,6})$	-0.222 (0.066)***	-0.165 (0.070)**	-0.167 (0.070)*	-0.192 (0.070)***
Mesh:mlgr$_{4.5}$	$(\beta_{11,7})$	NS	NS	NS	NS
Mesh:mlgr$_{5.0}$	$(\beta_{11,8})$	NS	NS	NS	NS
Mesh:mlgr$_{5.5}$	$(\beta_{11,9})$	NS	NS	NS	NS
Mesh:mlgr$_{6.0}$	$(\beta_{11,10})$	NS	NS	NS	NS
Mesh:mlgr$_{6.5}$	$(\beta_{11,11})$	NS	NS	NS	NS
Scale parameter	$(log\kappa)$	3.752 (0.402)***	3.058 (0.239)***	3.085 (0.247)***	3.049 (0.239)***
Proportion of deviance explained		0.900	0.892	0.891	0.890
Pearson's R^2 (observed vs. predicted)		0.838	0.787	0.792	0.789
AIC		1891	1929	1931	1937
ΔAIC			38	40	46

772

773

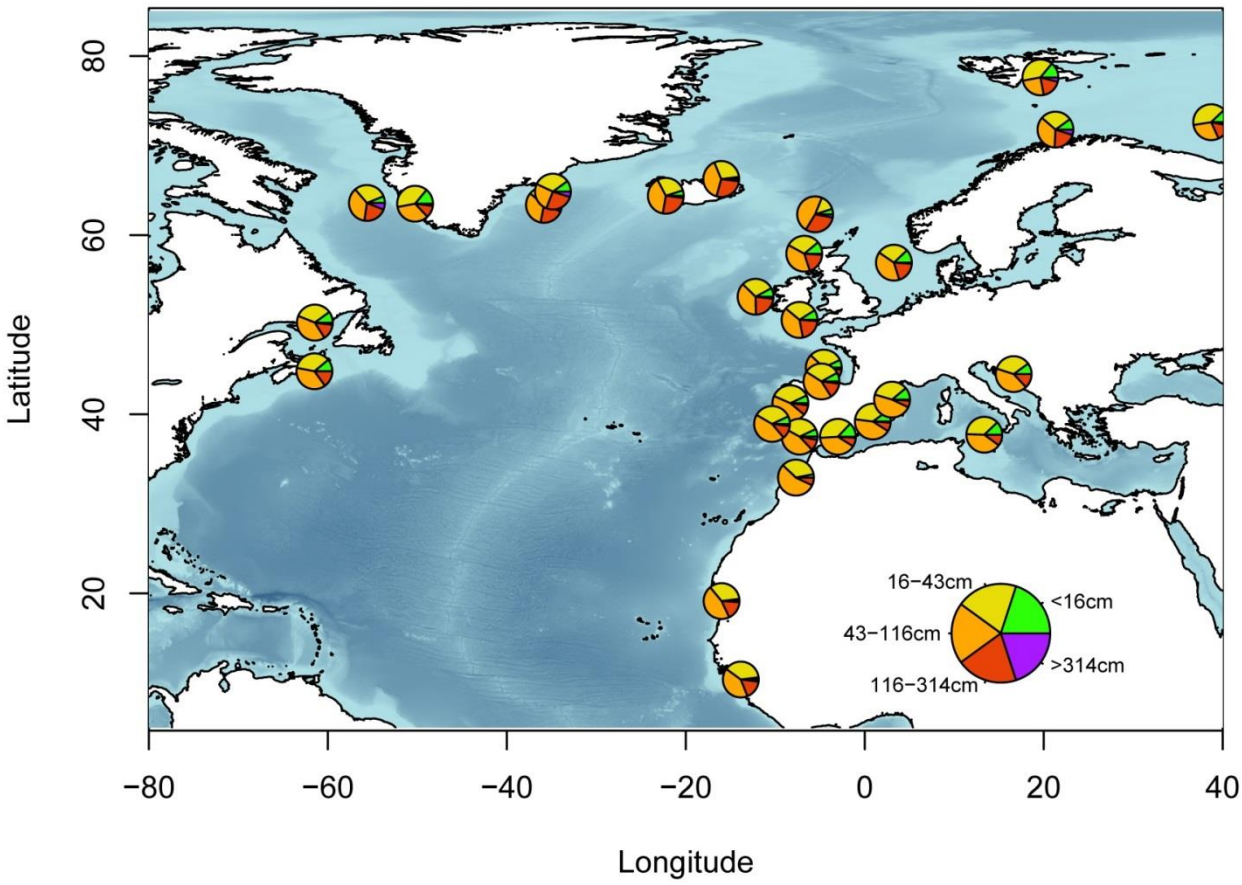

774

775 Figure 1. Pies showing the locations of the surveys and the relative number of species recorded in
776 each of the maximum length groups indicated in the lower right-hand corner of the map (plotted with
777 the R-package ‘marmap’).

778

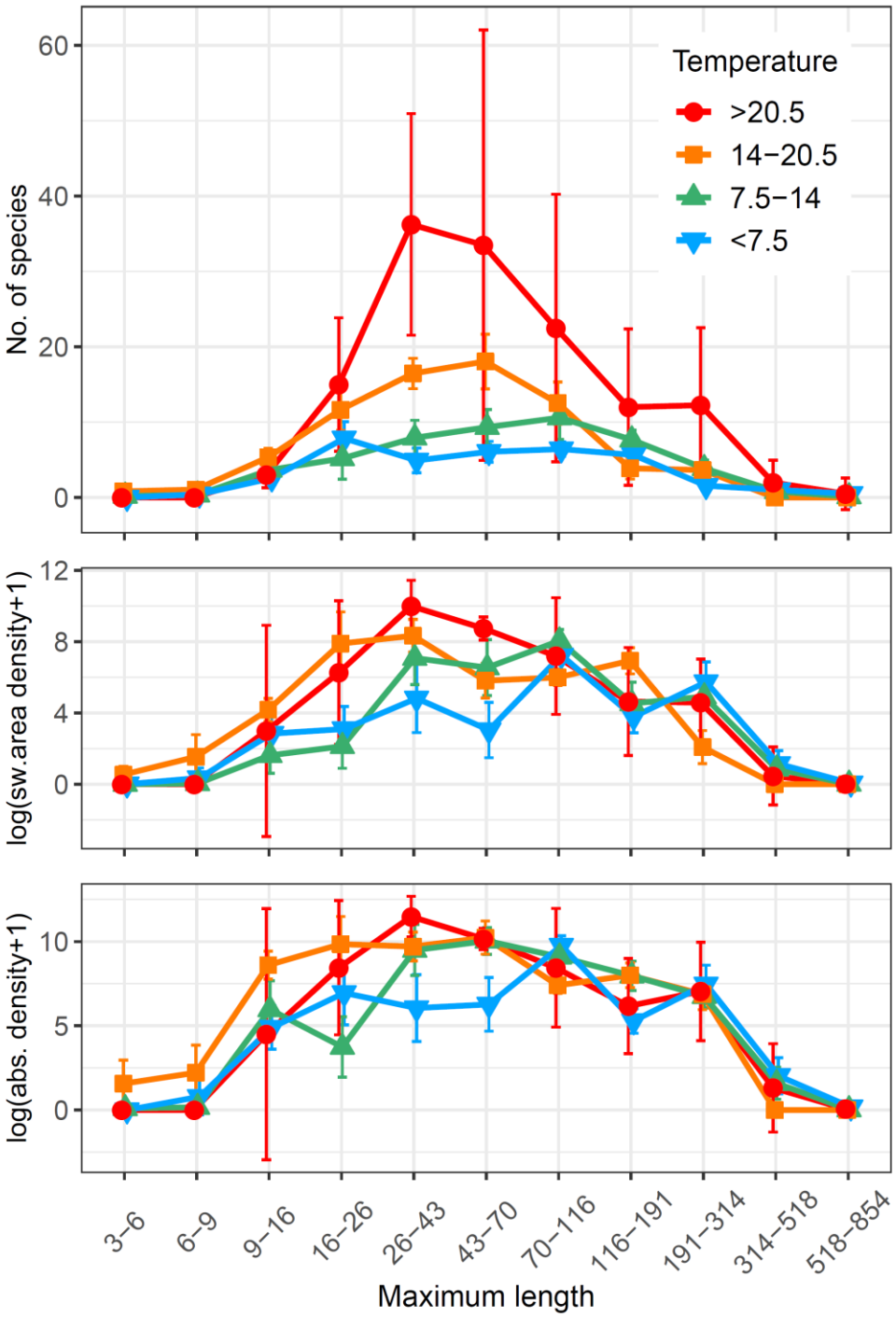

779

780 Figure 2. Average number of species, log swept area density (No*km^{-2}) and log absolute density
781 (No*km^{-2}) (±95% conf. limits) versus maximum length (cm) in four different sea surface temperature
782 intervals (°C).

Figure 3. Estimated smoothing curves from GAM using average sea temperature and other covariates to model the number of species observed by log maximum length group. Estimated degrees of freedom in brackets on the y-axis labels. Shaded area: 2*SE. Mesh-size smooths in bottom row only shown for three numerically abundant maximum length groups.

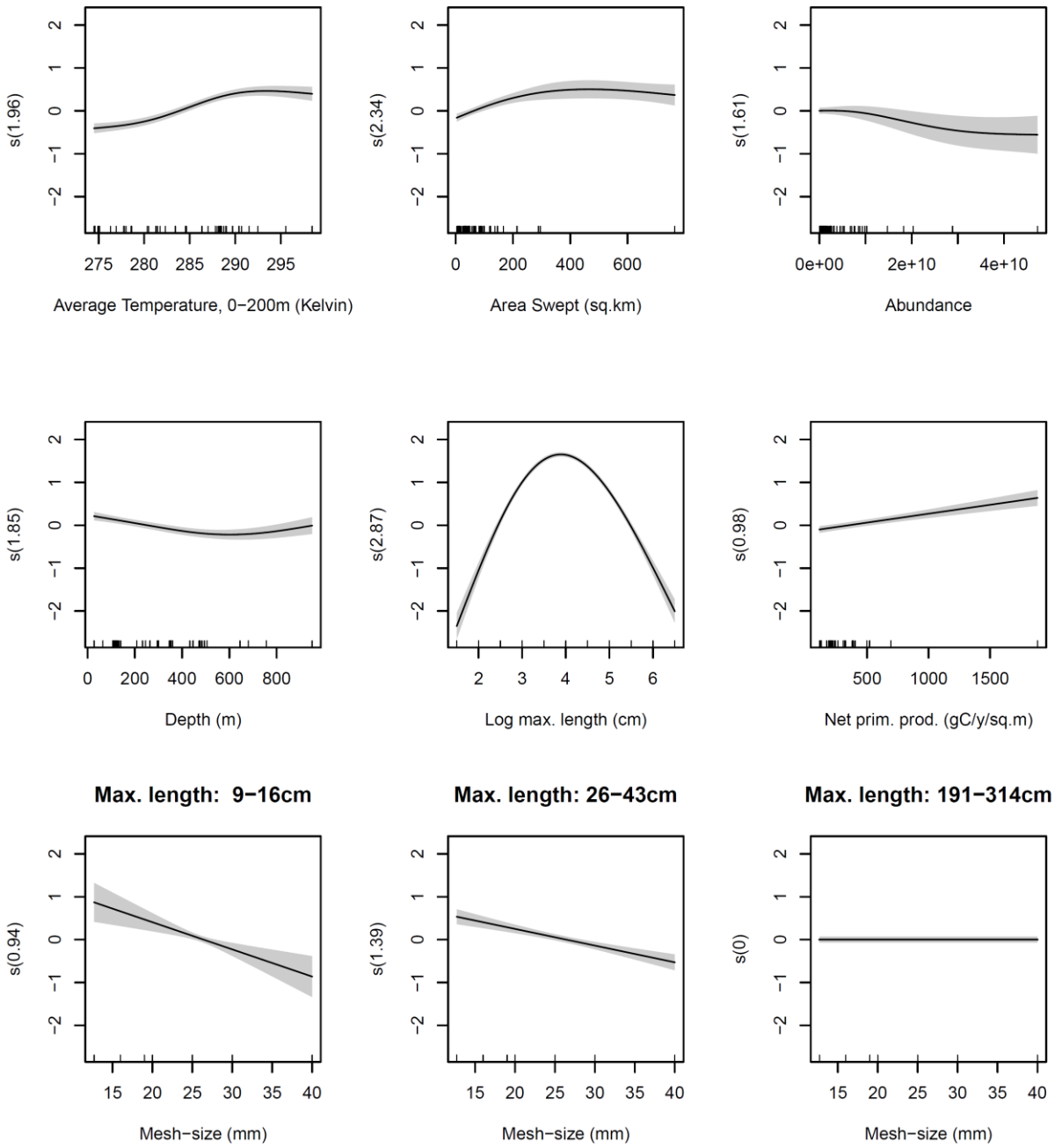

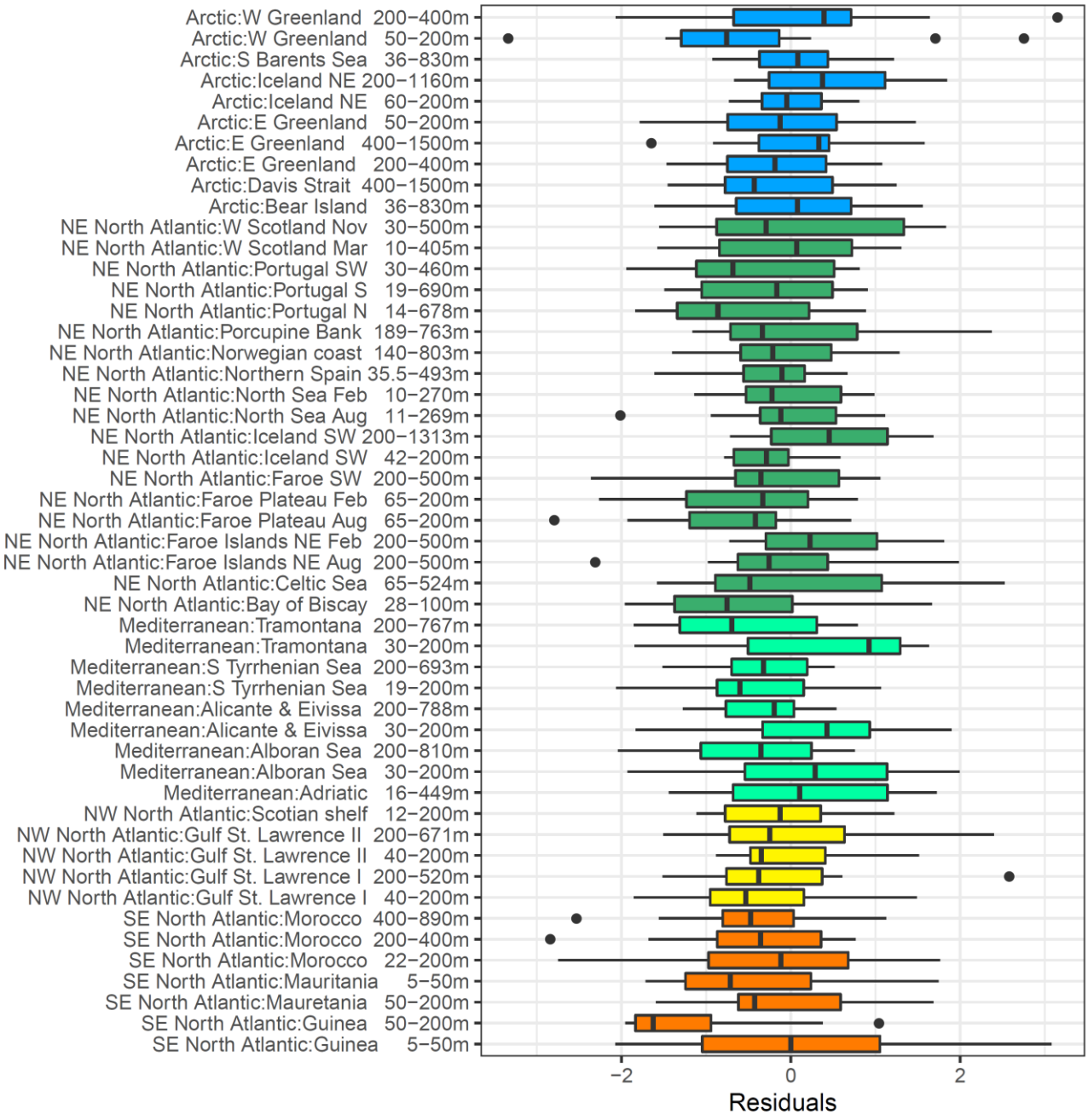

Figure 4. Box and whisker plot of log survey strata residuals from GAM model (box limits show 25% and 75% quartiles; the vertical bar in the middle of the box is the median of the residuals; whiskers show max. and min. values; and black dots are outliers; color indicate geographic regions).

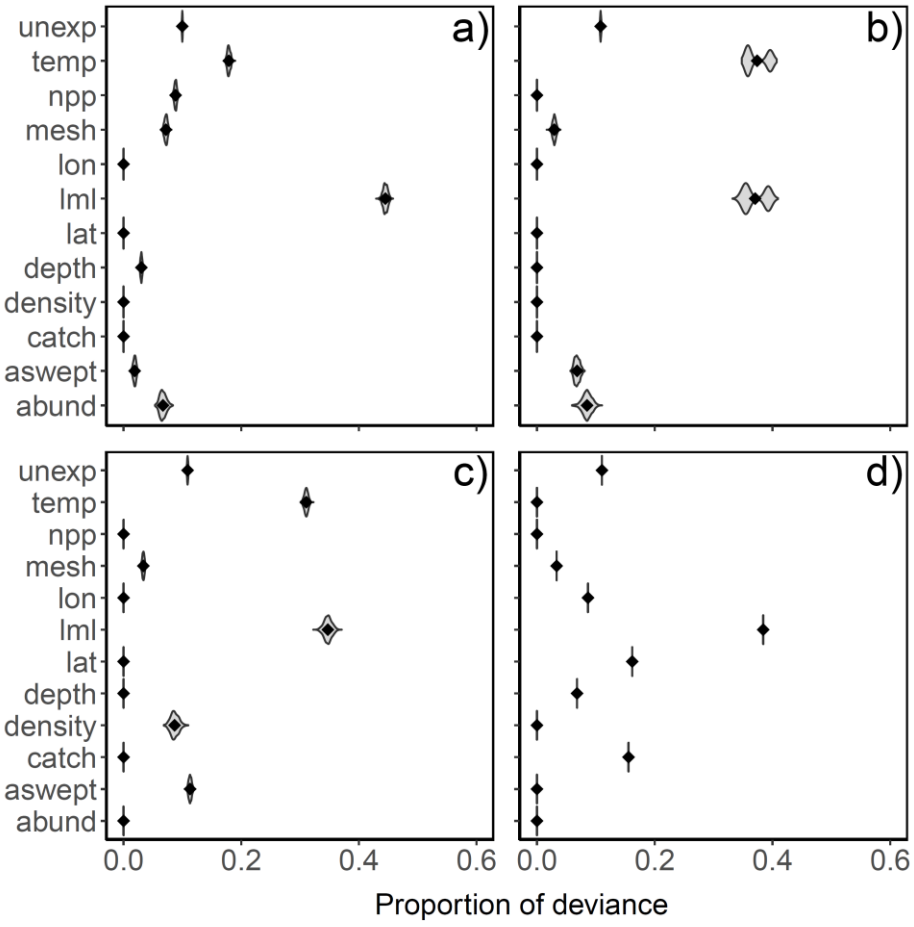

794

795

796 Figure 5.Violin plots of the relative contribution of the parameters in each of the four models to the
797 total deviance explained by each model. Results from 1000 non-linear model runs with stochastic
798 catchabilities. Unexplained deviance: unexp. Models: a) 'best' descriptive, b) neutral, c) metabolic, d)
799 environmental.